Environ. Sci. Technol. **2010,** *44,* 6954–6958

Oxidation Reactions Mediated by Single-Walled Carbon Nanotubes in Aqueous Solution

LEI REN[†] AND WENWAN ZHONG*[,†,‡]

Environmental Toxicology Graduate Program and Department of Chemistry, University of California, Riverside, California 92521

Received May 28, 2010. Revised manuscript received July 28, 2010. Accepted August 5, 2010.

How single-walled carbon nanotubes (SWCNT) function in redox reactions may be related to their behaviors in the induction of oxidative stress. Herein, oxidation of several biologically relevant reducing agents in the presence of SWCNT was studied in aqueous solutions. The selected reductants included a common indicator for intracellular reactive oxygen species (ROS) (2,7-dichlorodihydrofluorescein), small antioxidants (vitamin C, Trolox, and cysteine), and a high-molecular-weight ROS scavenger (bovine serum albumin). The unmodified or carboxylated SWCNT acted as both the oxidants and the catalysts in reactions. Moreover, they accelerated the oxidation reactions mediated by horseradish peroxidase, a representative member of the enzyme family actively involved in balancing oxidative stress. These diverse roles in redox reactions may serve the chemistry basis for SWCNT to induce oxidative stress in biological systems as potential environmental pollutants.

Introduction

Single-walled carbon nanotubes (SWCNT) have found applications in energy production, device miniaturization, sensor construction, and material fabrication, owing to their outstanding electrical, mechanical, and chemical properties. (*1*−*5*) However, the structural and morphological similarity of SWCNT to the carcinogenic asbestos fibers have raised tremendous concerns, (*6*) and more and more studies have been devoted to evaluate the impacts of SWCNT on health. (*7*−*10*) Still, an affirmative conclusion has not been reached, mostly because mechanisms governing the behaviors of SWCNT in biological systems are highly complex and could be relevant to the physicochemical properties of SWCNT as well as the diverse cellular defense pathways. In particular, whether and how SWCNT could induce oxidative stress is under debate. Oxidative stress was detected in cells invaded by SWCNT, (*8, 11*−*22*) judged from evidence like increased intracellular level of reactive oxygen species (ROS), glutathione depletion, decreased total antioxidant capacity, etc. (*18*−*22*) On the other hand, negligible oxidation damage was identified with SWCNT carrying supermolecular functionalization like dendrimers or drugs like amphotericin B and doxorubicin. (*23*−*26*)

Free radicals have been blamed for the induction of oxidative stress by SWCNT, (*17, 27, 28*) but only very few reports detected the presence of free radicals in SWCNT suspension. (*29*−*31*) Previously our group discovered that species with similar oxidation potentials as the peroxyl radicals may be produced in SWCNT solutions, because the SWCNT solution could oxidize ROS indicators for peroxyl radicals and the oxidations could only be quenched by peroxyl radical inhibitors. (*32*) The oxidation was positively related to the surface adsorption of oxygen, which may form 1,4-endoperoxide or 1,2-dioxetane via the addition of O_2 across a C_6-hexagon or to one C═C bond. (*33*) Moreover, it has been revealed that SWCNT in aqueous solutions could be oxidized or reduced by strong oxidants and reductants. (*34*−*38*) Hence, we continued to investigate how SWCNT were involved in the oxidation of ROS indicators and common antioxidants like vitamin C, Trolox, and free thiol-containing components. In addition, we explored the impact of SWCNT on oxidations mediated by horseradish peroxidase (HRP), a representative member of the enzyme family actively involved in balancing oxidative stress. Our results point out the possibility of SWCNT to consume antioxidants and affect reaction kinetics of peroxidase. Both may cause the imbalanced depletion of reducing scavengers in cells and consequently raise oxidative stress.

Experimental Section

Chemicals and Reagents. The present study focused on the unmodified and carboxylic acid-functionalized SWCNT (SWCNT-COOH). Both were obtained from Sigma and used as purchased. Information about the physical dimensions, functionalization, surface area, and metal impurity of SWCNT can be found in the Supporting Information, Table S1. HRP, ascorbic acid, bovine serum albumin (BSA), and 6-hydroxy-2,5,7,8-tetramethylchroman-2-carboxylic acid (Trolox) were purchased from Sigma (St. Louis, MO). Cysteine, 2,7-dichlorodihydrofluorescein diacetate (H_2DCF-DA), and the Thiol and Sulfide Quantitation Kit were obtained from Invitrogen (Eugene, OR).

SWCNT Preparation. Distribution of SWCNT in solutions was very important for SWCNT to exhibit their oxidation effects. Low oxidation capability was observed in the SWCNT-COOH samples prepared from a stock solution of 1 mg/mL (*32*), a concentration 10 times higher than the solubility of SWCNT-COOH in water (Figure S1). SWCNT aggregation occurred in the 1 mg/mL stock and significantly reduced the surface areas available for chemical reactions. To ensure good dispersion of SWCNT in the reaction solutions and preserve their oxidation power, in the present study, all SWCNT stocks were prepared in a concentration of 0.05 mg/mL with 1-h ultrasonication (100 W, 42 kHz). The unmodified SWCNT had very low solubility in water and thus 0.1% SDS was used as the dispersing agent.

Measurement of H_2DCF Oxidation by Fluorescence. Oxidation of H_2DCF was measured with the Victor II microplate reader (Perkin-Elmer, Waltham, MA). The H_2DCF stock solution was prepared on a daily basis by de-esterifying 20 nmol H_2DCF-DA with 0.25 mL of 0.01 M NaOH. Subsequently, 0.75 mL of 25 mM phosphate buffer (pH 7.4) was added to neutralized the resulted H_2DCF solution. In the oxidation study 10 μM H_2DCF was oxidized to DCF, which emitted strong fluorescence. Fluorescence intensities measured at various reaction time points were used to calculate the consumption of H_2DCF based on a calibration curve generated from DCF. Fluorescence quenching caused by SWCNT was adjusted by including SWCNT in the standard DCF solutions when acquiring the calibration curve.

* Corresponding author. E-mail: wenwan.zhong@ucr.edu. Fax: +1-951-827-4713.
† Environmental Toxicology Graduate Program.
‡ Department of Chemistry.

10.1021/es101821m

Published on Web 08/18/2010

H_2DCF Oxidation under Anaerobic and Aerobic Conditions Measured by UV−Vis−IR. Before mixing, the H_2DCF and SWCNT solutions were sealed separately, vacuumed for 25 min, and then purged with argon at 1 psi for more than 0.5 h. The two solutions were mixed in a tightly sealed cuvette. The final concentration for H_2DCF was 10 μM, and that of the unmodified SWCNT or SWCNT-COOH was 0.05 mg/mL. The absorbance spectrum from 400 to 1300 nm was measured at several reaction durations (1, 5, 10, 20, and 30 min) by the Cary 500 UV−vis−IR spectrometer (Varian, Palo Alto, CA). After 30 min, the cuvette was vacuumed for 15 min and exposed to air, and the UV−vis−IR spectrum was recorded at 10, 20, 30, 50, and 60 min.

Oxidation of Other Reducing Agents. Oxidation of ascorbic acid and Trolox by SWCNT-COOH was monitored in the Cary 500 UV−vis−IR spectrometer. The UV−vis−NIR spectra from 200 to 1300 nm simultaneously showed the quantity change of all reactants, including 56.8 μM ascorbic acid, 40.0 μM Trolox, and 0.05 mg/mL SWCNT-COOH. However, for comparing the oxidation rates of ascorbic acid and Trolox, the Cary 100 UV−vis spectrometer was used to observe only the changes in ascorbic acid and Trolox with a much faster scan rate. The residue thiol groups in cysteine and BSA after reacted with SWCNT was measured with the Thiol and Sulfide Quantitation Kit, following manufacturer's instruction.

Effect of SWCNT on the Reaction Kinetics of HRP. HRP (30 nM) and H_2O_2 (10 μM) were mixed in the microtiter plate wells with or without 0.007 mg/mL SWCNT. The reaction was initiated by rapidly adding H_2DCF to a final concentration of 5, 8, 10, 20, 50, 100, and 200 μM. The measurement and calculation of DCF concentrations were performed as described above. The initial rates of reactions were expressed as the amount of DCF produced per minute.

Result and Discussion

Duplex Roles of SWCNT in the Oxidation of H_2DCF. Even though our previous study on the oxidation of H_2DCF in aqueous suspension of SWCNT concluded that oxygen was the ultimate oxidant, residual oxidation of H_2DCF (~20%) was still observed under the anaerobic condition. Since SWCNT have been found to exist in both oxidized and reduced forms in aqueous solutions, (*34*) they may act as an oxidant and react with H_2DCF, which would generate changes in the near-infrared (NIR) spectrum of SWCNT-COOH. (*33, 39−41*) In the NIR spectrum, the regions between 1500−1800 nm (S_{11}) and 900−1100 nm (S_{22}) are features of semiconducting tubes and that located between 600−700 nm (M_{11}) corresponds to metallic tubes. (*41*) The absorption intensity of these regions would increase if SWCNT are reduced. Therefore, we collected the NIR spectra of SWCNT-COOH at different time points during the oxidation of H_2DCF to inspect how they participated in the reaction.

We first performed the reaction under anaerobic condition to avoid impact from O_2 (Figure 1A). Our SWCNT-COOH sample showed the central transition regions of S_{22} and M_{11} at 1040 and 700 nm, respectively, but the S_{11} transition which represents the lower energy band gap was not observed due to the large background interference from H_2O. The depletion of oxygen did not alter the oxidation status of SWCNT-COOH without H_2DCF, but the SWCNT-COOH was reduced immediately upon mixing with H_2DCF (Figure 1A). We monitored the change of absorbance (Abs.) at 498 nm (distinct for DCF generation) and 1040 nm (specific for SWCNT-COOH reduction) with time (insert in Figure 1B) and found out they were strongly correlated with each other ($R^2 = 0.994$; solid line in Figure 1B). This result indicates that, under anaerobic condition, SWCNT-COOH received electrons from H_2DCF as an oxidant. The originally low S_{22} transition band in SWCNT-COOH probably resulted from the strong acid

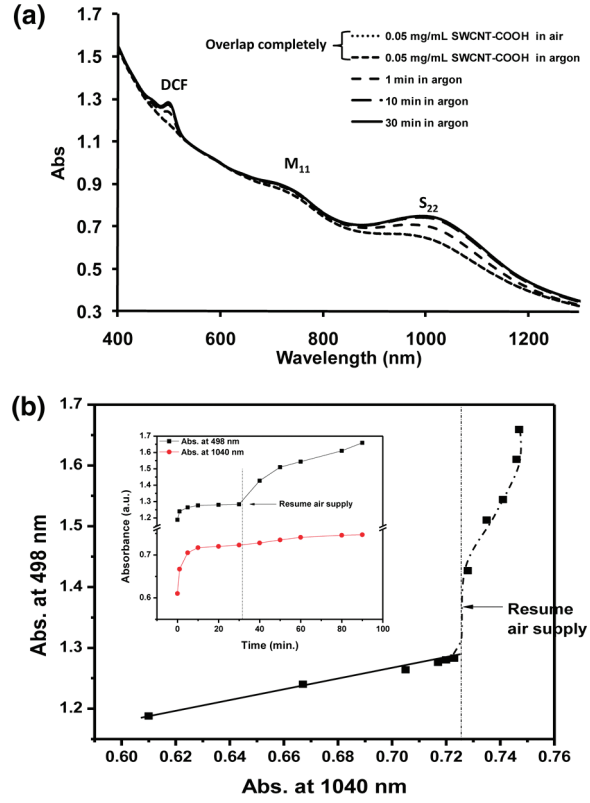

FIGURE 1. (A) UV−vis−IR spectra for oxidation of 10 μM H_2DCF in argon. Before and after purging air, the absorbance of 0.05 mg/mL SWCNT-COOH did not change. (B) The correlation between Abs at 498 and 1040 nm in the two reaction stages (anaerobic and aerobic). Insert: Abs at 498 nm by DCF and 1040 nm by SWCNT-COOH at 1, 10, and 30 min in argon as well as 10, 30, and 60 min after air supply was resumed.

treatment for the introduction of COOH group, (*42*) which likely exfoliated the tube, intercalated the acid into the graphite structure, and subsequently bleached the S_{22} band via the hole-doping effect. Adsorption of O_2 on SWCNT surface has also been claimed to impose such a hole-doping effect. (*43*) The pre-existing SWCNT-COOH doped by electron acceptors during manufacture and preprocessing was rapidly consumed to oxidize H_2DCF in the first 10 min, and the reaction slowed down when most of the doped SWCNT-COOH were consumed. Once we exposed the solution to air, the linear relationship between the Abs. at 498 and 1040 nm was disrupted suddenly with a much faster oxidation rate in H_2DCF than the reduction rate of SWCNT-COOH (dotted line in Figure 1B; spectra shown in Figure S2). Thus, under aerobic condition O_2 became the dominant oxidant in the reaction.

Similar reaction trends also occurred to the unmodified SWCNT (Figure S3A and B), but purging the solution with argon obviously increased the S_{22} absorbance even without the addition of H_2DCF (Figure S3A). The unmodified SWCNT were dispersed in 0.1% SDS by sonication. The coverage of SDS on the SWCNT surface may have weakened the binding of O_2, making it easier to be removed by argon, and also reduced the surface area for O_2 adsorption. Both led to a lower oxidation capability in the unmodified SWCNT than the SWCNT-COOH.

Clearly, SWCNT played two roles in the oxidation of H_2DCF: they themselves could be the oxidant and also could accelerate the reaction between O_2 and H_2DCF. SWCNT possesses ultra large surface area, and their adsorption of oxygen was calculated to be energetically favorable with ΔH equal to −16.3 kcal/mol. (*44*) The adsorbed oxygen on SWCNT surface may be added across the C=C bond and form

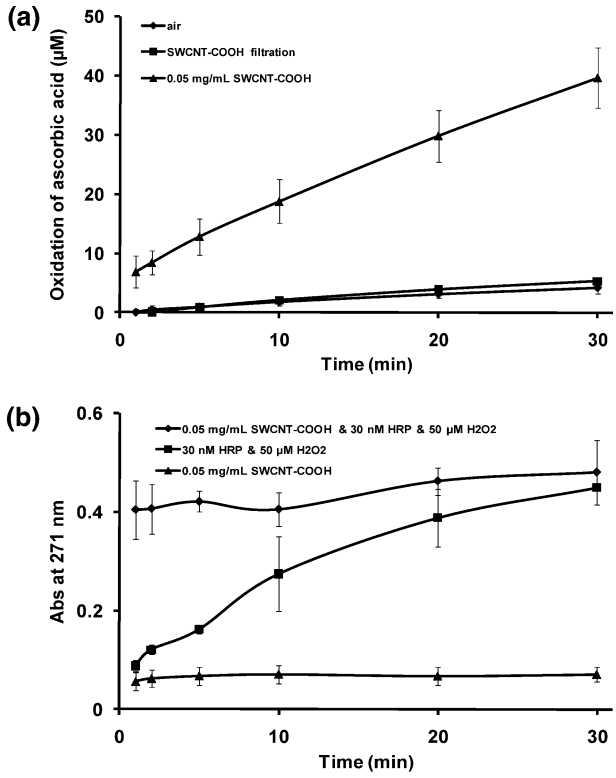

FIGURE 2. (A) Oxidation of vitamin C by air, 0.05 mg/mL SWCNT-COOH, or its equivalent-volume filtration; (B) oxidation of 40 μM Trolox by 0.05 mg/mL SWCNT-COOH, 30 nM HRP with 50 μM H_2O_2, as well as the mixture of SWCNT-COOH, HRP, and H_2O_2.

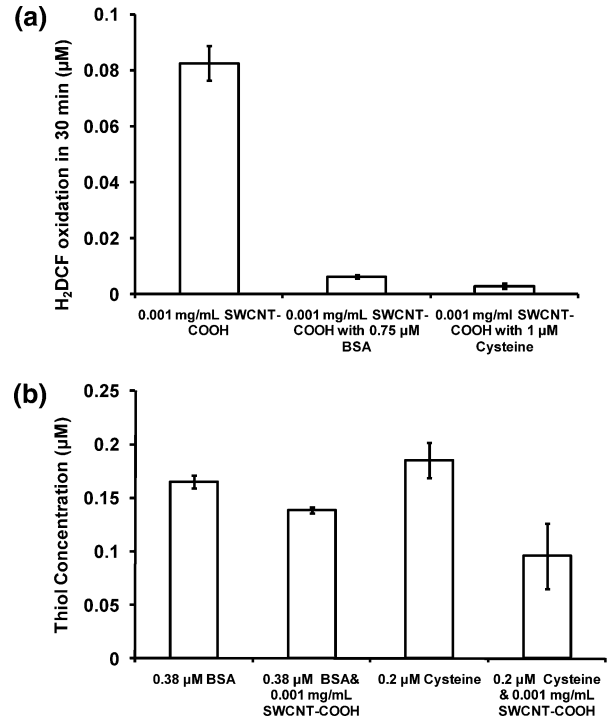

FIGURE 3. (A) inhibition effect of 0.75 μM BSA or 1 μM cysteine on the oxidation of 1 μM H_2DCF by 0.05 mg/mL SWCNT-COOH in 30 min. (B) The level of thiols in 0.38 μM BSA and 0.2 μM cysteine after exposure to 0.001 mg/mL SWCNT-COOH for 24 h.

transition species with reaction characteristics resemble to that of the peroxyl radical as revealed from our previous study. The adsorption-based activation of O_2 could also be the route via which SWCNT facilitate the oxidation of H_2DCF by O_2. Moreover, H_2DCF is an aromatic compound, and intercalation of aromatic compounds to SWCNT through $\pi-\pi$ stacking is well documented in literature. By adsorbing both the oxidant and reductant on the surface, SWCNT could speed up the electron transfer due to their high electron conductivity. (*45*)

Reactivity of SWCNT toward Other Reducing Molecules. The oxidation potential and catalytic capability shown by SWCNT in the oxidation of H_2DCF raised the question if they could react in the same ways with common antioxidants found in biological systems. Since vitamin C and Trolox, the water-soluble analog of tocopherol (vitamin E), were able to suppress the oxidation of H_2DCF by the unmodified SWCNT (*32*) and the SWCNT-COOH (Figure S4), we suspected that the inhibition effect might be due to the competition of oxidants in the reaction system. Indeed, the rate curves shown in Figure 2A indicated that the oxidation rate of vitamin C in the presence of 0.05 mg/mL SWCNT-COOH increased about 8 fold in comparison with that in air. The oxidation of vitamin C was monitored by the decrease of its characteristic absorption peak at 265 nm. SWCNT again acted as both the oxidant and the catalyst (Figure S5). No enhanced oxidation was observed if the SWCNT-COOH was removed from the solution by filtration. The presence of SWCNT-COOH was necessary for the oxidation reaction to occur. The reaction rate of vitamin C with SWCNT-COOH was faster than that of the H_2DCF. Within 30 min, 0.05 mg/mL SWCNT-COOH oxidized a total of 40 μM vitamin C but only produced around 5.3 μM DCF (data not shown), each molecule of vitamin C or H_2DCF losing 2 electrons in the redox reaction. The faster reaction rate of vitamin C supports that most of the oxygen species in the system could be consumed by vitamin C if it coexisted with H_2DCF, and consequently the oxidation of H_2DCF was suppressed.

However, the competition theory was not applicable to Trolox. Trolox suppressed the oxidation of H_2DCF in the SWCNT-COOH suspension within 30 min of reaction (Figure S4), but it stopped participating in the redox reaction after the reduction of SWCNT-COOH (Figures 2B and S6). Similarly, two free thiol containing antioxidants, BSA and cysteine exhibited immediate inhibition effects on the oxidation of H_2DCF in SWCNT-COOH solution (Figure 3A), but it took more than 24 h to oxidize the free thiol groups to a measurable level in these two molecules by SWCNT-COOH (Figure 3B). The suppression effect from BSA could be through the coating of SWCNT surface (*46*) which blocks the adsorption of oxygen and thus prevent the formation of the intermediate, epoxide-like species. However, the suppression mechanism of Trolox and cysteine was unknown.

Effect of SWCNT on the Activity of HRP. The reactivity of SWCNT over the common antioxidants may cause rapid depletion of these protecting molecules and break the intracellular redox balance if they enter the cells. However, cells are protected from oxidation damages by multiple pathways in addition to small antioxidants, and many of the pathways involve enzymes from the peroxidase family. Therefore, to further evaluate the impact of SWCNT reactivity on oxidation stress induction, we probed the possible influence of SWCNT on the function of peroxidase, using HRP as the model enzyme. Our measurement on the oxidation of H_2DCF (Figure S7) or Trolox (Figure 2B) by HRP/H_2O_2 clearly revealed that the reaction was accelerated by SWCNT-COOH. The reaction kinetics of HRP was then studied with or without the presence of SWCNT-COOH or unmodified SWCNT using H_2DCF as the substrate. The reaction catalyzed by HRP shows a ping-pong mechanism (*47*). The reaction kinetics with both H_2O_2 and H_2DCF as the substrates can be described with the following equation:

$$\frac{[HRP]_0}{v} = \frac{K_A}{k_{cat}}\frac{1}{[H_2DCF]} + \frac{1}{k_{cat}}\left(1 + \frac{K_B}{[H_2O_2]}\right)$$

in which $[HRP]_0$ is the total enzyme concentration, v is initial rate, K_A and K_B are Michaelis constants for H_2DCF and H_2O_2 respectively, and k_{cat} is the maximum theoretical rate constant. With a constant concentration of H_2O_2, $[HRP]_0/v$ is linearly proportional to $1/[H_2DCF]$. Figure 4 displays the curves obtained with HRP only, HRP plus SWCNT-COOH, and HRP plus unmodified SWCNT. Smaller slopes and intercepts were obtained with the two types of SWCNT. Assuming SWCNT has no impact on the K_B of H_2O_2, we could see that SWCNT-COOH increased the rate constant k_{cat} of the following reaction by a factor of 2.8 and decreased the K_A value of H_2DCF by a factor of 1.9. The unmodified SWCNT led to 2.1 fold reduction of k_{cat}, and 4.3 fold increases in K_A, Such changes indicated that oxidation of H_2DCF by the HRP complex II produced from the reaction between HRP and H_2O_2 was accelerated by SWCNT-COOH.

Two pieces of evidence made us believe that the above phenomena could be due to the facilitation of the long-range electron transfer between H_2DCF and HRP by SWCNT. One is the confirmation of direct interaction between HRP and SWCNT-COOH by CD measurement (Figure S8). HRP lost part of it α-helix secondary structure when mixed with SWCNT-COOH. (*48, 49*) The other is the inhibition behavior of Trolox on the oxidation of H_2DCF by the HRP/H_2O_2/SWCNT-COOH system. Trolox and H_2DCF occupied different binding sites on HRP so that it did not suppress the oxidation of H_2DCF by the HRP/H_2O_2 system. On the contrary, it inhibited the oxidation in the HRP/H_2O_2/SWCNT-COOH system (Figure S9). This result hints that SWCNT-COOH may enhance the electron transport between the heme group of HRP and the reductants. The binding site of Trolox on HRP may be closer to SWCNT surface and its electrons could then be routed to the heme group more easily, blocking the electron path of H_2DCF. Vitamin C does not bind to HRP, and thus the above phenomena were not observed with vitamin C (Figure S9). Facilitation of long-range electron transfer may also be the mechanism used by SWCNT to catalyze the reaction of antioxidants with oxygen. However, further investigation on the relative positions of key amino acids in HRP responsible for the electron migration (*45*) to the SWCNT-COOH surface is needed to confirm this hypothesis.

In summary, we demonstrated that SWCNT could oxidize the ROS indicator of H_2DCF and various antioxidants including vitamin C, cysteine, and BSA with different reaction rates in aqueous solution. The SWCNT could serve as the oxidant, and also facilitate the electron transport between the reducing agents and the oxidizing agents such as O_2 and HRP. The oxidation effect on the common ROS indicator emphasizes the importance of studying the oxidative stress in cells with different approaches besides the fluorescent microscopy with ROS indicators. The effects of SWCNT on the antioxidants and the peroxidase indicate that if SWCNT were taken up by the cells, they may enhance the cellular oxidative stress through the depletion of antioxidants and the augment of peroxidase activity. On the other hand, our results also point out that the chemical activity of SWCNT was dependent on their surface properties. Thus, adsorption of molecules present in biological systems, like proteins, onto SWCNT surface would increase the complexity of oxidative stress originated by SWCNT and should be taken into account when investigating the toxicity of SWCNT.

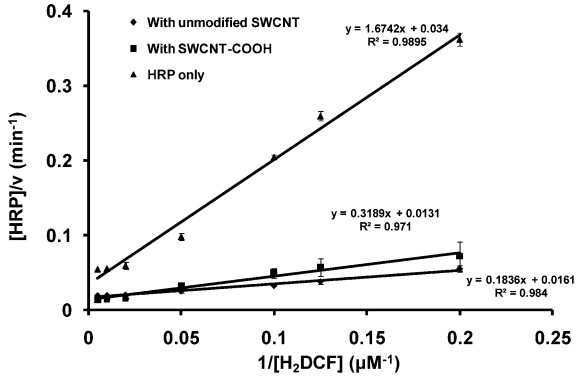

FIGURE 4. Kinetic of the H_2DCF oxidation by HRP with or without SWCNT. The concentration of enzyme and H_2O_2 were 30 nM and 10 μM, respectively. The concentrations of H_2DCF were 5, 8, 10, 20, 50, 100, and 200 μM.

Acknowledgments

The work was supported by the initial compliment provided to Dr. W. Zhong by the Department of Chemistry, University of California at Riverside. L.R. thanks the Environmental Toxicology Program for financial aid. The authors are also grateful to Mr. Tao Wu's assistance on collecting the BET data.

Supporting Information Available

Product information of the SWCNT used in our study is provided in Table S1. Oxidation of H_2DCF by SWCNT-COOH prepared in different concentrations is shown in Figure S1. Figure S2 displays the UV−vis−IR spectra for oxidation of H_2DCF by SWCNT-COOH in air. Oxidations of 10 μM H_2DCF by unmodified SWCNT in argon and in air are in Figure S3. Figure S4 depicts the inhibition effect of small molecules on H_2DCF oxidation by SWCNT-COOH. UV−vis−IR spectra for vitamin C and Trolox oxidation by SWCNT-COOH are found in Figure S5 and S6. Figure S7 shows the increased oxidation of H_2DCF in the system of SWCNT/HRP/H_2O_2, and Figure S8 contains the CD spectra of HRP with or without SWCNT-COOH. Figure S9 is the inhibition effect of small molecules on the oxidation of H_2DCF by SWCNT-COOH in the present of HRP. This material is available free of charge via the Internet at http://pubs.acs.org.

Literature Cited

(1) Dillon, A. C.; Jones, K. M.; Bekkedahl, T. A.; Kiang, C. H.; Bethune, D. S.; Heben, M. J. Storage of hydrogen in single-walled carbon nanotubes. *Nature* **1997**, *386* (6623), 377–379.

(2) Tans, S. J.; Verschueren, A. R. M.; Dekker, C. Room-temperature transistor based on a single carbon nanotube. *Nature* **1998**, *393* (6680), 49–52.

(3) Rutherglen, C.; Burke, P. Carbon nanotube radio. *Nano Lett.* **2007**, *7* (11), 3296–3299.

(4) Kong, J.; Franklin, N. R.; Zhou, C.; Chapline, M. G.; Peng, S.; Cho, K.; Dai, H. Nanotube molecular wires as chemical sensors. *Science* **2000**, *287* (5453), 622.

(5) Besteman, K.; Lee, J. O.; Wiertz, F. G. M.; Heering, H. A.; Dekker, C. Enzyme-coated carbon nanotubes as single-molecule biosensors. *Nano Lett.* **2003**, *3* (6), 727–730.

(6) Poland, C. A.; Duffin, R.; Kinloch, I.; Maynard, A.; Wallace, W. A. H.; Seaton, A.; Stone, V.; Brown, S.; MacNee, W.; Donaldson, K. Carbon nanotubes introduced into the abdominal cavity of mice show asbestos-like pathogenicity in a pilot study. *Nat. Nanotechnol.* **2008**, *3* (7), 423–428.

(7) Lam, C. W.; James, J. T.; McCluskey, R.; Hunter, R. L. Pulmonary toxicity of single-wall carbon nanotubes in mice 7 and 90 days after intratracheal instillation. *Toxicol. Sci.* **2004**, *77* (1), 126–134.

(8) Warheit, D. B.; Laurence, B. R.; Reed, K. L.; Roach, D. H.; Reynolds, G. A. M.; Webb, T. R. Comparative pulmonary toxicity assessment of single-wall carbon nanotubes in rats. *Toxicol. Sci.* **2004**, *77* (1), 117–125.

(9) Donaldson, K.; Aitken, R.; Tran, L.; Stone, V.; Duffin, R.; Forrest, G.; Alexander, A. Carbon nanotubes: a review of their properties in relation to pulmonary toxicology and workplace safety. *Toxicol. Sci.* **2006**, *92* (1), 5–22.

(10) Lam, C.; James, J. T.; McCluskey, R.; Arepalli, S.; Hunter, R. L. A review of carbon nanotube toxicity and assessment of potential occupational and environmental health risks. *Crit. Rev. Toxicol.* **2006**, *36* (3), 189–217.
(11) Kang, S.; Pinault, M.; Pfefferle, L. D.; Elimelech, M. Single-walled carbon nanotubes exhibit strong antimicrobial activity. *Langmuir* **2007**, *23* (17), 8670–8673.
(12) Manna, S. K.; Sarkar, S.; Barr, J.; Wise, K.; Barrera, E. V.; Jejelowo, O.; Rice-Ficht, A. C.; Ramesh, G. T. Single-Walled Carbon Nanotube Induces Oxidative Stress and Activates Nuclear Transcription Factor-kB in Human Keratinocytes. *Nano Lett.* **2005**, *5* (9), 1676–1684.
(13) Pacurari, M.; Yin, X. J.; Zhao, J.; Ding, M.; Leonard, S. S.; Schwegler-Berry, D.; Ducatman, B. S.; Sbarra, D.; Hoover, M. D.; Castranova, V. Raw Single-Wall Carbon Nanotubes Induce Oxidative Stress and Activate MAPKs, AP-1, NF-κB, and Akt in Normal and Malignant Human Mesothelial Cells. *Environ. Health Perspect.* **2008**, *116* (9), 1211.
(14) Shvedova, A. A.; Castranova, V.; Kisin, E. R.; Schwegler-Berry, D.; Murray, A. R.; Gandelsman, V. Z.; Maynard, A.; Baron, P. Exposure to nanotube material: assessment of nanotube cytotoxicity using human keratinocyte cells. *J. Toxicol. Environ. Health, Part A* **2003**, *20* (66), 1909–1926.
(15) Tian, F.; Cui, D.; Schwarz, H.; Estrada, G. G.; Kobayashi, H. Cytotoxicity of single-wall carbon nanotubes on human fibroblasts. *Toxicol. Vitro* **2006**, *20* (7), 1202–1212.
(16) Jia, G.; Wang, H.; Yan, L.; Wang, X.; Pei, R.; Yan, T.; Zhao, Y.; Guo, X. Cytotoxicity of carbon nanomaterials: single-wall nanotube, multi-wall nanotube, and fullerene. *Environ. Sci. Technol.* **2005**, *39* (5), 1378–1383.
(17) Pulskamp, K.; Diabat, S.; Krug, H. F. Carbon nanotubes show no sign of acute toxicity but induce intracellular reactive oxygen species in dependence on contaminants. *Toxicol. Lett.* **2007**, *168* (1), 58–74.
(18) Grabinski, C.; Hussain, S.; Lafdi, K.; Braydich-Stolle, L.; Schlager, J. Effect of particle dimension on biocompatibility of carbon nanomaterials. *Carbon* **2007**, *45* (14), 2828–2835.
(19) Herzog, E.; Byrne, H. J.; Davoren, M.; Casey, A.; Duschl, A.; Oostingh, G. J. Dispersion medium modulates oxidative stress response of human lung epithelial cells upon exposure to carbon nanomaterial samples. *Toxicol. Appl. Pharmacol.* **2009**, *236* (3), 276–281.
(20) Mueller, L.; Riediker, M.; Wick, P.; Mohr, M.; Gehr, P.; Rothen-Rutishauser, B. Oxidative stress and inflammation response after nanoparticle exposure: differences between human lung cell monocultures and an advanced three-dimensional model of the human epithelial airways. *J. R. Soc., Interface* **2010**, *7* (Suppl. 1), S27–S40.
(21) Sharma, C. S.; Sarkar, S.; Periyakaruppan, A.; Barr, J.; Wise, K.; Thomas, R.; Wilson, B. L.; Ramesh, G. T. Single-walled carbon nanotubes induces oxidative stress in rat lung epithelial cells. *J. Nanosci. Nanotechnol.* **2007**, *7* (7), 2466–2472.
(22) Yang, H.; Liu, C.; Yang, D.; Zhang, H.; Xi, Z. Comparative study of cytotoxicity, oxidative stress and genotoxicity induced by four typical nanomaterials: the role of particle size, shape and composition. *J. Appl. Toxicol.* **2009**, *29* (1), 69–78.
(23) Lacerda, L.; Bianco, A.; Prato, M.; Kostarelos, K. Carbon nanotubes as nanomedicines: from toxicology to pharmacology. *Adv. Drug Delivery Rev.* **2006**, *58* (14), 1460–1470.
(24) Prato, M.; Kostarelos, K.; Bianco, A. Functionalized carbon nanotubes in drug design and discovery. *Acc. Chem. Res.* **2008**, *41* (1), 60–68.
(25) Liu, D.; Yi, C.; Zhang, D.; Zhang, J.; Yang, M. Inhibition of Proliferation and Differentiation of Mesenchymal Stem Cells by Carboxylated Carbon Nanotubes. *ACS Nano* **2010**, *4* (4), 2185–2195.
(26) Zhang, Y.; Ali, S. F.; Dervishi, E.; Xu, Y.; Li, Z.; Casciano, D.; Biris, A. S., Cytotoxicity Effects of Graphene and Single-Wall Carbon Nanotubes in Neural Phaeochromocytoma-Derived PC12 Cells. *ACS Nano*, ACS ASAP.
(27) Kagan, V. E.; Tyurina, Y. Y.; Tyurin, V. A.; Konduru, N. V.; Potapovich, A. I.; Osipov, A. N.; Kisin, E. R.; Schwegler-Berry, D.; Mercer, R.; Castranova, V. Direct and indirect effects of single walled carbon nanotubes on RAW 264.7 macrophages: Role of iron. *Toxicol. Lett.* **2006**, *165* (1), 88–100.
(28) Guo, L.; Morris, D. G.; Liu, X.; Vaslet, C.; Hurt, R. H.; Kane, A. B. Iron bioavailability and redox activity in diverse carbon nanotube samples. *Chem. Mater.* **2007**, *19* (14), 3472–3478.
(29) Fenoglio, I.; Tomatis, M.; Lison, D.; Muller, J.; Fonseca, A.; Nagy, J. B.; Fubini, B. Reactivity of carbon nanotubes: Free radical generation or scavenging activity. *Free Radical Biol. Med.* **2006**, *40* (7), 1227–1233.
(30) Chen, Y.; Chen, J.; Hu, H.; Hamon, M. A.; Itkis, M. E.; Haddon, R. C. Solution-phase EPR studies of single-walled carbon nanotubes. *Chem. Phys. Lett.* **1999**, *299* (6), 532–535.
(31) Lin, A. M. Y.; Chyi, B. Y.; Wang, S. D.; Yu, H. H.; Kanakamma, P. P.; Luh, T. Y.; Chou, C. K.; Ho, L. T. Carboxyfullerene prevents iron-induced oxidative stress in rat brain. *J. Neurochem.* **2001**, *72* (4), 1634–1640.
(32) Ren, L.; Kim, H. K.; Zhong, W. Capillary electrophoresis-assisted identification of peroxyl radical generated by single-walled carbon nanotubes in a cell-free system. *Anal. Chem.* **2009**, *81* (13), 5510.
(33) Dukovic, G.; White, B. E.; Zhou, Z.; Wang, F.; Jockusch, S.; Steigerwald, M. L.; Heinz, T. F.; Friesner, R. A.; Turro, N. J.; Brus, L. E. Reversible surface oxidation and efficient luminescence quenching in semiconductor single-wall carbon nanotubes. *J. Am. Chem. Soc.* **2004**, (126), 15269–15276.
(34) Zheng, M.; Diner, B. A. Solution redox chemistry of carbon nanotubes. *J. Am. Chem. Soc.* **2004**, *126* (47), 15490.
(35) Zheng, M.; Rostovtsev, V. V. Photoinduced charge transfer mediated by DNA-wrapped carbon nanotubes. *J. Am. Chem. Soc.* **2006**, *128* (24), 7702–7703.
(36) Hu, C.; Zhang, Y.; Bao, G.; Zhang, Y.; Liu, M.; Wang, Z. L. DNA functionalized single-walled carbon nanotubes for electrochemical detection. *J. Phys. Chem. B* **2005**, *109* (43), 20072–20076.
(37) Napier, M. E.; Hull, D. O.; Thorp, H. H. Electrocatalytic oxidation of DNA-wrapped carbon nanotubes. *J. Am. Chem. Soc.* **2005**, *127* (34), 11952–11953.
(38) Song, C.; Pehrsson, P. E.; Zhao, W. Recoverable solution reaction of HiPco carbon nanotubes with hydrogen peroxide. *J. Phys. Chem. B* **2005**, *109* (46), 21634–21639.
(39) Strano, M. S.; Huffman, C. B.; Moore, V. C.; O Connell, M. J.; Haroz, E. H.; Hubbard, J.; Miller, M.; Rialon, K.; Kittrell, C.; Ramesh, S. Reversible, band-gap-selective protonation of single-walled carbon nanotubes in solution. *J. Phys. Chem. B* **2003**, *107* (29), 6979–6985.
(40) Xu, Y.; Pehrsson, P. E.; Chen, L.; Zhao, W. Controllable redox reaction of chemically purified DNA- single walled carbon nanotube hybrids with hydrogen peroxide. *J. Am. Chem. Soc.* **2008**, *130* (31), 10054–10055.
(41) Itkis, M. E.; Perea, D. E.; Niyogi, S.; Rickard, S. M.; Hamon, M. A.; Hu, H.; Zhao, B.; Haddon, R. C. Purity evaluation of as-prepared single-walled carbon nanotube soot by use of solution-phase near-IR spectroscopy. *Nano Lett.* **2003**, *3* (3), 309–314.
(42) Khairutdinov, R. F.; Itkis, M. E.; Haddon, R. C. Light Modulation of Electronic Transitions in Semiconducting Single Wall Carbon Nanotubes. *Nano Lett.* **2004**, *4* (8), 1529–1533.
(43) Moonoosawmy, K. R.; Kruse, P. Cause and Consequence of Carbon Nanotube Doping in Water and Aqueous Media. *J. Am. Chem. Soc.* **2010**, *132*, 1572–1577.
(44) Da Silva, A. M.; Junqueira, G. M. A.; Anconi, C. P. A.; Dos Santos, H. F. New insights on chemical oxidation of single-wall carbon nanotubes: a theoretical study. *J. Phys. Chem. C* **2009**, *113* (23), 10079–10084.
(45) Saito, T.; Matsuura, K.; Ohshima, S.; Yumura, M.; Iijima, S. Long-Range Electron Transfer through a Single-walled Carbon Nanotube Sheet. *Adv. Mater.* **2008**, *20* (13), 2475–2479.
(46) Valenti, L. E.; Fiorito, P. A.; Garcia, C. D.; Giacomelli, C. E. The adsorption-desorption process of bovine serum albumin on carbon nanotubes. *J. Colloid Interface Sci.* **2007**, *307* (2), 349–356.
(47) Dunford, H. B. *Horseradish Peroxidase: Structure and Kinetic Properties In Peroxidases in Chemistry and Biology Vol. II*; Everse, J., Everse, K. E., Grisham, M. B., Eds.; CRC Press: Boca Raton, FL, 1991; p 5.
(48) Adak, S.; Mazumder, A.; Banerjee, R. K. Probing the active site residues in aromatic donor oxidation in horseradish peroxidase: involvement of an arginine and a tyrosine residue in aromatic donor binding. *Biochem. J.* **1996**, *314*, 985–991.
(49) Chattopadhyay, K.; Mazumdar, S. Structural and conformational stability of horseradish peroxidase: effect of temperature and pH. *Biochemistry* **2000**, *39* (1), 263–270.

ES101821M